POLITECNICO DI TORINO
Repository ISTITUZIONALE

Joint Graph-Based User Scheduling with LFoV Beamforming Design for B5G/6G NTN Systems

Original
Joint Graph-Based User Scheduling with LFoV Beamforming Design for B5G/6G NTN Systems / Dakkak, M.R., Riviello, D.G., Guidotti, A., Vanelli-Coralli, A.. - ELETTRONICO. - (2025), pp. 212-217. (14th IEEE-APS Topical Conference on Antennas and Propagation in Wireless Communications, APWC 2025 Palermo (Ita) 08-12 September 2025) [10.1109/APWC65665.2025.11190467].

Availability:
This version is available at: 11583/3016496 since: 2026-10-10T13:15:51Z

Publisher:
IEEE

Published
DOI:10.1109/APWC65665.2025.11190467

Terms of use:

This article is made available under terms and conditions as specified in the corresponding bibliographic description in the repository

Publisher copyright
IEEE postprint/Author's Accepted Manuscript

©2025 IEEE. Personal use of this material is permitted. Permission from IEEE must be obtained for all other uses, in any current or future media, including reprinting/republishing this material for advertising or promotional purposes, creating new collecting works, for resale or lists, or reuse of any copyrighted component of this work in other works.

(Article begins on next page)

22 October 2026

Joint Graph-based User Scheduling with LFoV Beamforming Design For B5G/6G NTN Systems

M. Rabih Dakkak*, Daniel Gaetano Riviello†, Alessandro Guidotti‡, Alessandro Vanelli-Coralli*
*Dept. of Electrical, Electronic, and Information Engineering (DEI), Univ. of Bologna, Bologna, Italy
†CNR-IEIIT, Consiglio Nazionale delle Ricerche, Istituto di Elettronica e di Ingegneria dell'Informazione e delle Telecomunicazioni, Torino, Italy
‡National Inter-University Consortium for Telecommunications (CNIT), Univ. of Bologna Research Unit, Italy
daniel.riviello@cnr.it, {mrabih.dakkak2, a.guidotti, alessandro.vanelli}@unibo.it

***Abstract*—In this paper, we study the problem of user scheduling for Low Earth Orbit (LEO) Multi-User (MU) Multiple-Input-Multiple-Output (MIMO) Non-Terrestrial Network (NTN) systems with the objective of maximizing the sum-rate capacity while minimizing the total number of clusters. We propose graph-based scheduling based on Iterative Maximum Independent Set Search and Removal (IMISSR) with a constant graph user density integrated with Limited Field of View (LFoV) Subarray beamforming design based on Signal-to-Leakage-and-Noise Ratio (SLNR). Users are grouped together based on the channel coefficient of correlation (CoC) as dissimilarity metric and served by the satellite via Space Division Multiple Access (SDMA) by means of the proposed digital beamforming design on a cluster basis. Clusters are then served in different time slots via Time Division Multiple Access (TDMA). The results, presented in terms of per-cluster sum-rate capacity and per-user throughput, show that the presented joint approach of IMISSR with LFoV BF design can significantly improve the system performance w.r.t. the benchmark schedulers.**

***Index Terms*—LEO, MU-MIMO, User Scheduling, Beamforming, MMSE**

I. Introduction

Non-Terrestrial Networks (NTNs) are becoming increasingly important in the evolution of 5G and beyond towards 6G due to their ability to provide service continuity, ubiquity, and scalability. They can provide long-range coverage for areas like rural and remote locations, and furthermore in emergencies or natural disaster involving public safety where Terrestrial Networks (TNs) coverage encounter limitations [1]. In the context of 6G, NTNs are expected to assume an even more pivotal role by enabling "anything, anytime, anywhere" connectivity, thereby bridging the digital divide and connecting the unconnected. The study of NTNs in 5G began with 3GPP Release 17, continued through Release 18 and 19 for enhancements in 5G-Advanced, and is progressing in Releases 20 and 21 to further develop NTN capabilities while paving the way for 6G standardization. [2]. Recently, the planning of Low Earth Orbit (LEO) satellites, commonly known as mega-constellations or, more broadly, Non-Geostationary Orbit (NGSO) systems, has obtained high interest from the research and industry, due to its advantage to have short propagation delays compared to the Geostationary Orbit (GEO) systems [2]. The scarcity of spectrum resources to meet the increased demanding requirements of future communication B5G/6G systems is considered one of the main challenges. To this aim, several strategies are proposed aiming at efficient utilization of the available spectrum bandwidth through either dynamic spectrum utilization schemes, such as Cognitive Radio solutions [3], [4], or by fully exploiting the spectrum by decreasing the frequency reuse factor down to Full Frequency Reuse (FFR) [5]. However, the latter solution introduces substantial Co-Channel Interference (CCI), thus necessitating the use of advanced interference management techniques at the transmitter side, e.g., beamforming (BF), Multi-User-Multiple Input Multiple Output (MU-MIMO), and Radio Resourse Management (RRM). The authors in these studies [5]–[9], provided a thorough overview of beamforming techniques in NTNs for both GSO and NGSO constellations. The emphasis has centered on improving data rates in unicast and/or multicast systems, alongside addressing challenges related to NTN-based beamforming, such as scheduling algorithms and Channel State Information (CSI) recovery. To address the challenges of complexity and cost of phased antenna arrays, the introduction of subarrayed configurations has been identified as a key solution, as intoduced in [11]. This approach has also been implemented MU-MIMO systems in [12]. The authors in [13] proposed a design for beamforming algorithms for MU-MIMO in LEO systems that use multiple subarrays. In this design, each subarray is controlled by a single radio frequency (RF) chain. This approach reduces the number of beamforming ports required and, as a result, lessens the on-board processing demands. In [14], the authors present an architecture for Limited Field of View (LFoV) arrays that operate within a very narrow steering range. To address the challenge of having a greater number of User Terminals (UTs) than the available transmit antennas on the satellite, user scheduling becomes essential in NTN. This scheduling can be implemented through either user selection or user grouping techniques. The first option focuses on identifying a specific subset from the pool of all available users, while user grouping algorithms categorize all users into groups that are served during consecutive time slots. User grouping presents an NP-complete problem, which is typically resolved through exhaustive search methods such as approximation algorithms or heuristic ones [15]. In [16], the authors assess the design of user scheduling metrics for Downlink (MU-MIMO) systems accommodating various users. They propose two hybrid user

scheduling algorithms aimed at achieving a balance between fairness among users and maximizing overall capacity through a greedy approach. Based on this work, the authors in [17] introduce a novel computationally efficient algorithm called Multiple Antenna Downlink Orthogonal Clustering (MADOC) that will be utilized as a reference approach in our analysis.

In this paper, we develop and merge our previous works [18], [19] by proposing graph-based scheduling based on Iterative Maximum Independent Set Search and Removal (IMISSR) combined with LFoV subarray design considering Signal-to-Leakage-and-Noise Ratio (SLNR) as a beamformer in MIMO LEO NTN systems. We perform an heuristic optimization of the graph density value, which maximizes the sum-rate capacity. We show that the proposed approach can significantly improve the performance w.r.t. the reference schedulers and beamformer without subarraying.

II. System Model

We assume a single multi-beam LEO satellite at altitude $h_{sat} = 600$ km provided with an on-board planar antenna array of N_{tot} radiating elements organized into N subarrays, giving connection to K uniformly distributed on-ground UEs through S beams ($S < N$ and $S \ll K$). As stated earlier, FFR is supposed to be used, resulting in all beams utilizing identical spectral resources. To ensure user connectivity, the LEO satellite shall establish a logical connection with an on-ground gNB. To achieve this, the satellite is presumed to be directly linked to a ground-based gateway (GW), as shown in Fig. 1. The considered system model architecture

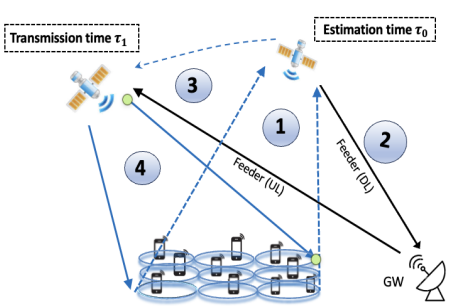

Fig. 1: System Architecture.

is thoroughly described in [18], [19]. The RRM scheduling and beamforming coefficients are computed at the on-ground gNB. This computation requires the estimates CSI which are performed by the UEs. As illustrated in Fig. 1, the estimates are calculated at a time instant τ_0, when the satellite is located at a specified position in its orbit. Afterwards, the estimates are returned to the network entity, i.e., the GW, to calculate the scheduling and beamforming coefficients for every group of users. Such coefficients are provided to the satellite. Then, the actual beamformed symbols are transmitted to the users at time instant $\tau_0 + \Delta\tau$. The time delay $\Delta\tau$ occurring between the phase of channel estimation and the phase of transmission causes a misalignment between the channel utilized for computing the beamforming and scheduling matrices and the actual channel for transmission, thereby affecting the performance of the system. The delay is given

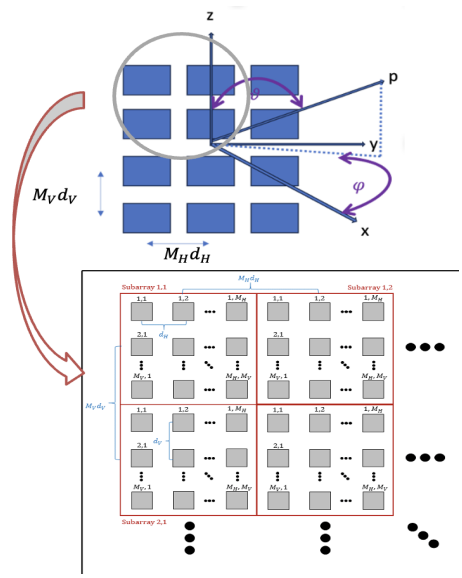

Fig. 2: Coordinate system for the Uniform Planar Array model.

as follows: $\Delta\tau = \tau_{user} + \tau_{feeder}^{(UL)} + \tau_{feeder}^{(DL)} + \tau_p + \tau_{ad}$; where: i) τ_{user} is is the latency on the user return link; ii) $\tau_{feeder}^{(DL)}$ is the delay on the feeder downlink iii) $\tau_{feeder}^{(UL)}$ is the delay on the feeder uplink iv) τ_p is the processing delay required to compute the beamforming coefficients; and finally τ_{ad} defines any additional latency.

A. Antenna architecture and channel model

The antenna model and the array geometry are based on ITU-R Recommendation M.2101-0 [20](Fig. 2). Generally, the antenna boresight direction points to the Sub Satellite Point (SSP), while the point **P** represents the position of the user terminal on the ground. The user direction can be identified by the angle pair (ϑ, φ) where the boresight direction is (0,0). The direction cosines for the considered user can be expressed as: $u = \frac{P_y}{||\mathbf{P}||}\sin\vartheta\sin\varphi$, and $v = \frac{P_z}{||\mathbf{P}||}\cos\vartheta$. The overall array response of the Uniform Planar Array (UPA) made of subarrays in the direction (ϑ_i, φ_i) for user i can be expressed as the Kronecker product between the two array responses of the Uniform Linear Arrays (ULAs) lying on the y-axis and z-axis. Let us first define the $1 \times N_{\text{H}}$ Steering Vector (SV) of the ULA along the y-axis, $\mathbf{a}_{\text{H}}(\theta_i, \varphi_i)$, and the $1 \times N_{\text{V}}$ SV of the ULA along the z-axis, $\mathbf{a}_{\text{V}}(\theta_i)$ [21]:

$$\mathbf{a}_{\text{H}}(\vartheta_i, \varphi_i) = \left[1, e^{jk_0 M_{\text{H}} d_{\text{H}} \sin\vartheta_i \sin\varphi_i}, \ldots, e^{jk_0 M_{\text{H}} d_{\text{H}} (N_{\text{H}}-1) \sin\vartheta_i \sin\varphi_i}\right] \tag{1}$$

$$\mathbf{a}_{\text{V}}(\vartheta_i) = \left[1, e^{jk_0 M_{\text{V}} d_{\text{V}} \cos\vartheta_i}, \ldots, e^{jk_0 M_{\text{V}} d_{\text{V}} (N_{\text{V}}-1) \cos\vartheta_i}\right] \tag{2}$$

where $k_0 = 2\pi/\lambda$ is the wave number, $N_{\text{H}}, N_{\text{V}}$ denote the number of subarrays on the horizontal and vertical directions, respectively, with $N = N_{\text{H}} N_{\text{V}}$, and $M_{\text{H}}, M_{\text{V}}$ denote the number of antenna elements per each subarray on the horizontal (y-axis) and vertical (z-axis) directions, respectively, with $M = M_{\text{H}} M_{\text{V}}$, and finally $d_{\text{H}}, d_{\text{V}}$ denote the distance between adjacent antenna elements on the horizontal and vertical directions, respectively, as shown in Fig. 2. It is worth mentioning that

the total number of antenna elements are $N_{tot} = MN$, where $M = 1$ if subarraying is not implemented. We can define the total steering vector of the full UPA (an array equipped with subarrays as antenna elements) as the Kronecker product of the 2 SV's along each axis: $\mathbf{a}_{\text{UPA}}(\vartheta_i, \varphi_i) = \mathbf{a}_{\text{H}}(\vartheta_i, \varphi_i) \otimes \mathbf{a}_{\text{V}}(\vartheta_i)$. We further assume that the satellite is equipped with directive antenna elements, whose radiation pattern is denoted by $g_{\text{E}}(\vartheta_i, \varphi_i)$ according to Table 3 in [20], and these elements are grouped in N subarrays of size $M_{\text{H}} \times M_{\text{V}}$. It is worth recalling that a LFoV array has no steering nor beamforming capabilities at antenna element level, but only at subarray level; for this reason, the linear phase shifts of the SVs in (1) and (2) are taken w.r.t. the center of each subarray. We can define the subarray factor $F_{sub}(\vartheta_i, \varphi_i)$ as:

$$F_{sub}(\vartheta_i, \varphi_i) = \frac{\sin\left(\frac{M_{\text{V}}}{2} k_0 d_{\text{V}} \cos\vartheta_i\right)}{\sqrt{M_{\text{V}}} \sin\left(\frac{1}{2} k_0 d_{\text{V}} \cos\vartheta_i\right)} \frac{\sin\left(\frac{M_{\text{H}}}{2} k_0 d_{\text{H}} \sin\vartheta_i \sin\varphi_i\right)}{\sqrt{M_{\text{H}}} \sin\left(\frac{1}{2} k_0 d_{\text{H}} \sin\vartheta_i \sin\varphi_i\right)}. \tag{3}$$

Finally, we can express the total SV of the UPA of subarrays made of directive antenna elements at the satellite targeted for the i-th user as the product between the full UPA $\mathbf{a}_{\text{UPA}}(\vartheta_i, \varphi_i)$, the element radiation pattern, and the subarray factor:

$$\mathbf{a}(\vartheta_i, \varphi_i) = g_{\text{E}}(\vartheta_i, \varphi_i) F_{sub}(\vartheta_i, \varphi_i)\, \mathbf{a}_{\text{UPA}}(\vartheta_i, \varphi_i). \tag{4}$$

The CSI vector, $\mathbf{h}_i$ represents the channel between the N radiating elements and the generic i-th on-ground UE, with $i = 1, ...K$, and can be written as:

$$\mathbf{h}_i = G_i^{(rx)} \frac{\lambda}{4\pi d_i} \sqrt{\frac{L_i}{\kappa B T_i}} e^{-j\frac{2\pi}{\lambda} d_i} \mathbf{a}(\vartheta_i, \varphi_i) \tag{5}$$

where: i) d_i is the slant range between the i-th user and the satellite,; ii) $\kappa B T_i$ refers the equivalent thermal noise power, with κ being the Boltzmann's constant, B is the user bandwidth which is assumed to be the same for all users, and T_i is the equivalent noise temperature of the i-th user receiver; iii) L_i denotes the additional losses per user (e.g., atmospheric and antenna cable losses), and iv) $G_i^{(rx)}$ denotes the receiving antenna gain for the i-th UE. The additional losses are computed as $L_i = L_{sha,i} + L_{atm,i} + L_{sci,i}$, where $L_{sha,i}$ represents the log-normal shadow fading term, $L_{atm,i}$ the atmospheric loss, and $L_{sci,i}$ the scintillation, these terms are computed as per 3GPP TR 38.821 [22].

B. Radio Resource Management and KPIs

By collecting all of the K CSI vectors, it is possible to build a $K \times N$ complex channel matrix at system level $\hat{\mathbf{H}} = \left[\hat{\mathbf{h}}_1^{\intercal}, \hat{\mathbf{h}}_2^{\intercal}, \ldots, \hat{\mathbf{h}}_K^{\intercal}\right]^{\intercal}$, where the generic k-th row contains the CSI vector of the k-th user and the generic n-th column contains the channel coefficients from the n-th on-board feed towards the K on-ground users. Given the set of all users to be scheduled, denoted with $\mathcal{U} = \{U_1, U_2, \ldots, U_K\}$, the RRM algorithm defines a possible users' partitioning $\{\mathcal{C}_1, \mathcal{C}_2, \ldots, \mathcal{C}_P\}$ where $\mathcal{C}_p \subseteq \mathcal{U}$ is defined as cluster and $|\mathcal{C}_p| = K_p$ is defined as the cardinality of the p-th cluster with $p = 1, \ldots, P$. In order to minimize the the total number of clusters P, we further assume that each user can be assigned only to one cluster (as in [17], [19]), therefore clusters are disjoint sets of users, $\mathcal{C}_i \cap \mathcal{C}_j = \varnothing,\ \forall i, j$. In each time slot, users belonging to cluster $\mathcal{C}_p$ are selected, leading to a $K_p \times N$ complex scheduled channel matrix $\hat{\mathbf{H}}_p \subseteq \hat{\mathbf{H}}$, which contains only the rows of the scheduled users in the p-th cluster. The selected beamforming algorithm computes for each cluster a $N \times K_p$ complex beamforming matrix $\mathbf{W}_p = [\mathbf{w}_1^{(p)}, \mathbf{w}_2^{(p)}, \ldots, \mathbf{w}_{K_p}^{(p)}]$, where $\mathbf{w}_i^{(p)}$ denotes the $N \times 1$ beamformer designed for the i-th user in the p-th cluster. The matrix $\mathbf{W}_p$ projects the K_p dimensional column vector $\mathbf{s}_p = [s_1, s_2, \ldots, s_{K_p}]^{\intercal}$ containing the unit-variance users' symbols onto the N-dimensional space. Thus, in the feed space, the computation of the beamforming matrix allows for the generation of a dedicated beam towards each user direction. The signal received by the i-th user in the p-th cluster can be expressed as follows [19]:

$$y_k^{(p)} = \mathbf{h}_k \mathbf{w}_k^{(p)} s_k + \sum_{\substack{i=1 \\ i \neq k}}^{K_p} \mathbf{h}_k \mathbf{w}_i^{(p)} s_i + z_k^{(p)} \tag{6}$$

The K_p-dimensional vector of received symbols in the p-th cluster is

$$\mathbf{y}_p = \mathbf{H}_p \mathbf{W}_p \mathbf{s}_p + \mathbf{z}_p \tag{7}$$

where $\mathbf{W}_p$ is the scheduling and the beamforming matrices in the estimation phase (τ_0), while at a time instant $\tau_0 + \Delta t$, in which the scheduled channel matrices and vectors are different and denoted as $\mathbf{H}_p$ and $\mathbf{h}_k$, respectively. The SINR for user k belonging to cluster p can be computed as

$$\text{SINR}_k^{(p)} = \frac{\left\|\mathbf{h}_k \mathbf{w}_k^{(p)}\right\|^2}{1 + \sum_{\substack{i=1 \\ i \neq k}}^{K_p} \left\|\mathbf{h}_k \mathbf{w}_i^{(p)}\right\|^2} \tag{8}$$

Given a TDMA time frame T_F, each cluster is assigned a time slot T_p. In order to design a fair-proportional scheduler, we assume that we can adjust the duration of each time slot T_p to be proportional to the cardinality of each cluster K_p, i.e.,

$$T_p = \gamma_p T_F \qquad , \qquad \gamma_p = \frac{K_p}{\sum_{p=1}^{P} K_p} = \frac{K_p}{K} \tag{9}$$

since each user can be assigned to only one cluster. Therefore, in order to take into account the duty cycle associated with each cluster, we can define the per-user throughput as:

$$R_k = \gamma_p B \log_2\left(1 + \text{SINR}_k^{(p)}\right) \tag{10}$$

where γ_p denotes the cluster weight. We finally define the per-cluster sum-rate capacity as an additional KPI independent of the cluster weight:

$$\Gamma_p = B \sum_{k=1}^{K_p} \log_2(1 + \text{SINR}_k^{(p)}) \tag{11}$$

C. Beamforming and power normalization

The beamforming matrix $\mathbf{W}_p$, which is computed on a cluster basis, is based on the linear Minimum Mean Square Error (MMSE) equation:

$$\mathbf{W}_p = \hat{\mathbf{H}}_p^H (\hat{\mathbf{H}}_p \hat{\mathbf{H}}_p^H + \alpha \mathbf{I}_{K_p})^{-1} \tag{12}$$

where $\mathbf{I}_{K_p}$ indicates the $K_p \times K_p$ identity matrix and $\alpha = \frac{N}{P_t}$ is the regularisation factor with P_t the total on-board power. Under the assumptions of single-antenna users and Equal Power Allocation (EPA), i.e, each user is assigned the same amount of power from P_t, we can obtain the formula of the Signal-to-Leakage-plus-Noise Ratio (SLNR) beamformer $\hat{\mathbf{W}}_p$ by normalizing the columns of MMSE beamformer as follows [23]:

$$\hat{\mathbf{W}}_p = \frac{1}{\sqrt{N_F}} \mathbf{W}_p (\text{diag}(\text{diag}(\mathbf{W}_p^H \mathbf{W}_p)))^{-\frac{1}{2}} \tag{13}$$

It should be noted that the power emitted by the satellite and the antenna in beamforming is a particularly challenging step and needs careful consideration [8]. For this work, we considered the Sum Power Constraint (SPC) and the Per-Antenna Power Constraint (PAPC) [4] to obtain the normalized beamforming matrix, as follows:

$$\tilde{\mathbf{W}}_p^{(SPC)} = \frac{\sqrt{P_t}\hat{\mathbf{W}}_p}{\sqrt{\text{tr}(\hat{\mathbf{W}}_p \hat{\mathbf{W}}_p^H)}} \tag{14}$$

$$\tilde{\mathbf{W}}_p^{(PAPC)} = \sqrt{\frac{P_t}{N_F}} \hat{\mathbf{W}}_p (\text{diag}(\text{diag}(\hat{\mathbf{W}}_p \hat{\mathbf{W}}_p^H)))^{-\frac{1}{2}} \hat{\mathbf{W}}_p \tag{15}$$

III. Scheduling algorithms:

We denote by $\mathcal{G} = (\mathcal{V}, \mathcal{E})$ an undirected and unweighted graph with vertex set $\mathcal{V}$ and edge set $\mathcal{E}$. In our scheduling scenario, the set of vertices $\mathcal{V}$ coincides with the set of users $\mathcal{U}$ and the edge set is constructed based on the channel Coefficient of Correlation (CoC) [15], [17], defined as:

$$[\mathbf{\Psi}]_{i,j} = \frac{\left|\mathbf{h}_i \mathbf{h}_j^H\right|}{\|\mathbf{h}_i\| \, \|\mathbf{h}_j\|} \tag{16}$$

where $[\mathbf{\Psi}]_{i,j} \in [0, 1]$. The set of edges $\mathcal{E}$ of the $\mathcal{G}$ graph is completely determined by its adjacency matrix $\mathbf{A}$, whose entries are defined as:

$$[\mathbf{A}]_{i,j} = \begin{cases} 1, & [\mathbf{\Psi}]_{i,j} \geq \delta_{th} \\ 0, & [\mathbf{\Psi}]_{i,j} < \delta_{th} \end{cases} \tag{17}$$

for $i \neq j$, while $[\mathbf{A}]_{i,i} = 0, \ \forall i$, i.e., $\mathcal{G}$ has no self-loops; δ_{th} denotes the graph threshold. An edge between U_i and U_j implies that their channels $\mathbf{h}_i$ and $\mathbf{h}_j$ are considered nearly co-linear and therefore they cannot be co-scheduled. The graph threshold determines the density of the graph $D(\mathbf{\Psi}, \delta_{th})$ which can be computed as

$$D(\mathbf{\Psi}, \delta_{th}) = \frac{2|\mathcal{E}_c|}{|\mathcal{V}| \left(|\mathcal{V}| - 1\right)} = \frac{1}{2} \sum_{i=1}^{K} \sum_{j=1}^{K} [\mathbf{A}]_{i,j} \tag{18}$$

An independent set in a graph $\mathcal{G}$ is a subset of the vertices $\mathcal{I} \subseteq \mathcal{U}$ such that there is no pair of adjacent vertices $U_i, U_j \in \mathcal{I}$. A maximum independent set $\mathcal{I}_{\text{max}}$ is an independent set of largest possible size for a given graph $\mathcal{G}$. Please notice that the maximum independent set in graph $\mathcal{G}$ corresponds to the maximum clique, i.e., the largest complete subgraph, in the complement graph $\overline{\mathcal{G}}$ (where adjacent vertices become non-adjacent, and non-adjacent vertices become adjacent). The proposed grouping technique, called Iterative Maximum Independent Set Search and Removal (IMISSR), aims at finding $\mathcal{I}_{\text{max}}$ at each iteration, pruning the users belonging to $\mathcal{I}_{\text{max}}$ from $\mathcal{G}$ and reconstructing the graph according to a target graph density, until no more users are left to be scheduled.

Algorithm 1 IMISSR with constant graph density.

Require: Set of users $\mathcal{U}$, channel CoC matrix $\mathbf{\Psi}$ and target graph density ϵ_t
Initialize $p = 1$ and $K = |\mathcal{U}|$
while $\mathcal{U} \neq \varnothing$ **do**
  δ_{th} = BisectionMethod($\mathbf{\Psi}$, 0, 1, ϵ_t, tol, T_{max})
  $\mathcal{I}_{\text{max}}$ = FindMIS($\mathbf{A}$)
  $\mathcal{C}_p \leftarrow \mathcal{I}_{\text{max}}$
  $K_p \leftarrow |\mathcal{C}_p|$
  Remove all rows and columns of $\mathbf{\Psi}$ associated with users in $\mathcal{I}_{\text{max}}$
  $\mathcal{U} \leftarrow \mathcal{U} - \mathcal{I}_{\text{max}}$
  $K \leftarrow K - K_p$
  $\gamma_p = \frac{K_p}{K}$
  $p \leftarrow p + 1$
end while
procedure BisectionMethod($\mathbf{\Psi}$, a, b, ϵ_t, tol, T_{max})
  $c = \frac{a+b}{2}$ and $i = 0$
  while $|D(\mathbf{\Psi}, c) - \epsilon_t| > tol \ \ \& \ \ i < T_{\text{max}}$ **do**
    if $(D(\mathbf{\Psi}, b) - \epsilon_t) \cdot (D(\mathbf{\Psi}, c) - \epsilon_t) < 0$ **then**
      $a = c$
    else
      $b = c$
    end if
    $c = \frac{a+b}{2}$
    $i \rightarrow i + 1$
  end while
  return c
end procedure

Finding the maximum independent set is a strong NP-hard problem, therefore we have to resort to a heuristic greedy approach. As illustrated in Alg. 1, we design a scheduling algorithm that aims at minimizing the total number of clusters P and maximizing the average per-user throughput. The iterative procedure searches for the maximum independent set $\mathcal{I}_{\text{max}}$ through the efficient and simple heuristic FindMIS [24], and declares it as a cluster; at each step the nodes in $\mathcal{I}_{\text{max}}$ and any edges connected to them are removed, the graph is reconstructed in order to match a desired density of the graph as in (18). Similar to [19], we first set a constant target graph density value ϵ_t, then at each step (both at the beginning and after each pruning), we search for the threshold δ_{th} such that $D(\mathbf{\Psi}, \delta_{th}) = \epsilon_t$. To obtain the respective threshold value for the required target density ϵ_t, we aim at finding the root of the function $D(\mathbf{\Psi}, \delta_{th}) - \epsilon_t$ through the bisection method [25]. Within this method, the root to be found is initially bounded between 0 and 1, the search interval is repeatedly halved until convergence is reached through the parameter tol. Finally, the parameter T_{max} limits iterations to prevent infinite loops. The heuristic FindMIS [24] is also a greedy iterative algorithm, in which the maximum independent set is found by removing at each step the vertex with the highest degree (largest number of neighbors), and in case of multiple vertices with the same highest degree, the vertex with the highest support is removed, which is the sum of the degrees of all neighboring vertices.

A. Benchmark scheduling algorithms

1) MADOC: Multiple Antennas Downlink Orthogonal Clustering, [17], which uses the CoC matrix as a metric to find ϵ-orthogonal user groups, i.e., groups of users in which

the CoC does not exceed a predefined threshold ϵ_t which is optimized to maximize the overall capacity of the system.

2) Position-based scheduler: the users are scheduled based on their location. Specifically, a beam lattice is generated on ground only for scheduling purposes, as shown in Fig. 3, and a single user is randomly selected for each beam at each time slot; the total number of time slots is determined to ensure that every user is served at least once.

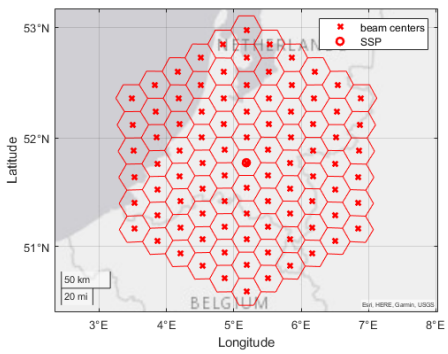

Fig. 3: Generated beam lattice for position-based scheduler.

IV. Numerical Results

TABLE I: Simulation parameters.

Parameter	Value	Parameter	Value
Carrier frequency	20 GHz	Propagation scenario	Line of Sight
System band	400 MHz	Total on-board power density, $P_{t,\text{dens}}$	4 dBW/MHz
Beamforming space	feed	Total on-board power density with subarraying	$P_{t,\text{dens}} - 10\log_{10}(M_{\text{H}}M_{\text{V}})$
Receiver type	VSAT		
Receiver antenna gain	39.7 dBi	Number of scheduled users K_{sch}	91
Noise figure	1.2 dB	Number of subarrays N	1024 (32 $\times$32)
Coverage area	101077 km^2	Num of elements per each subarray M	(2 $\times$ 2)
User density	0.05 user/km^2	Number of antenna elements without subarraying	$N_{tot} = N$= 1024
System scenario	urban	Num of antenna elements with subarraying	$N_{tot} = MN$= 4096

In this section, we present the outcomes of the extensive numerical simulations with the parameters specified as in Tab. I. The assessment is performed in full buffer conditions, i.e., infinite traffic demand. A single LEO satellite is considered at a distance of 600 Km from the Earth. On average the total number of users is $K = 2850$. In order to have a fair comparison, the transmitted power in case of subarrayed BF has been divided by $(M_{\text{H}}M_{\text{V}})$, i.e., the maximum achievable subarray gain, so that the EIRP for both subarrayed and non-subarrayed cases shall be equivalent. Since a LFoV array has no steering capability at antenna-level, no hybrid beamforming is taken into account.

In all simulations, we observe that the performance of the proposed IMISSR scheduling algorithm outperforms the reference MADOC scheduler and significantly surpasses the position-based scheduler for both SLNR-SPC and SLNR-PAPC beamforming with subarrays design. Aiming at maximizing the total sum-rate capacity by scheduling porocess, we performed a heuristic optimization of the graph density, and we obtained optimized thresholds for the proposed IMISSR and the reference MADOC scheduler for both SLNR-SPC and SLNR-PAPC as shown in Tab. II. It is evident that the IMISSR with LFoV subarrys BF design has the highest

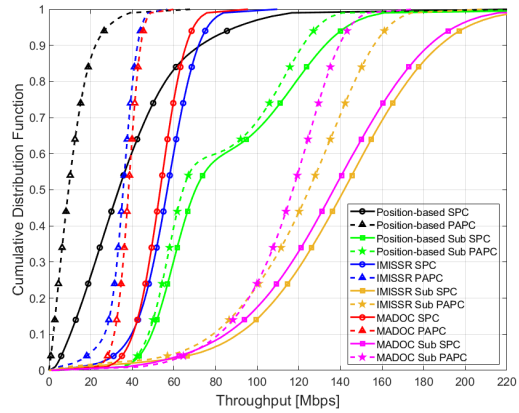

Fig. 4: CDF of the users' throughput.

average per-cluster sum-rate capacity (Gbps), and mean cluster size as compared to the other schedulers. And if we compare the performance of subarrayed and non-subarrayed analysis, shown in Tab. II, we can note that the high obtained gain by proposing LFoV architecture for all the analyzed schedulers.

TABLE II: Numerical results for all scheduling algorithms.

BF architecture and power normalization		Position-based	MADOC	IMISSR
Average user throughtput [Mbps]				
Non-subarrayed	SPC	38.2	53.2	55.99
	PAPC	11.18	37.87	34.68
Subarrayed	SPC	83.79	135	139.63
	PAPC	78.45	113.38	119.91
Average per-cluster sum-rate capacity [Gbps]				
Non-subarrayed	SPC	136.38	187.35	194.81
	PAPC	39.92	132.7	119.23
Subarrayed	SPC	299.11	462.39	483.82
	PAPC	280.03	387.26	404.77
Mean cluster size				
Non-subarrayed	SPC	91	54.12	57.84
	PAPC	91	40	47.96
Subarrayed	SPC	91	181.9	186.35
	PAPC	91	140.23	150.85
Optimized threshold				
Non-subarrayed	SPC	—	0.52	0.045
	PAPC	—	0.33	0.067
Subarrayed	SPC	—	0.66	0.012
	PAPC	—	0.52	0.019

The Cumulative Distribution Function (CDF) of user throughput in Fig. 4 demonstrates that the IMISSR with SLNR-SPC achieves an average throughput improvement of 2.79 Mbps over MADOC in non-subarrayed configurations, and a 4.6 Mbps gain in scenarios without subarrayed design. Fig 5 illustrates the CDF of the per-cluster sum-rate capacity across all considered schedulers. It is observed that only 8% of clusters with IMISSR achieve less than 300 Gbps combined with Subarrayed SLNR-SPC, whereas this percentage increases to 14% and 23% when using the reference MADOC and position-based schedulers, respectively. Finally, it is worth emphasizing that the beamforming design with LFoV subarrying is performing much better for all the

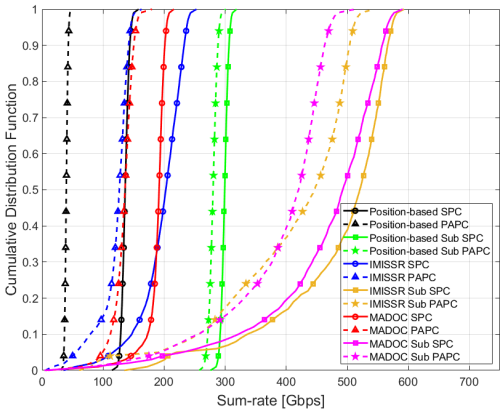

Fig. 5: CDF of the per-cluster sum-rate capacity.

analyzed schedulers compared to reference design without subarrys which is motivated by the fact the LFoV subarray design has improved directivity, i.e., it produces narrower beams over the service area. Consequently, enhances the interference rejection capability of the proposed techniques.

V. Conclusion

In this paper, we addressed the problem of user scheduling for LEO Multi-User (MU-MIMO) NTN systems with the objective of maximizing the sum-rate capacity while minimizing the total number of clusters. We propose graph-based scheduling based on Iterative Maximum Independent Set Search and Removal (IMISSR) with a constant graph user density integrated with Limited LFoV Subarray beamforming design based SLNR. The results, presented in terms of per-cluster sum-rate capacity and per-user throughput, show that the presented joint approach of IMISSR with LFoV BF design can significantly improve the system performance w.r.t. the benchmark MADOC and position-based schedulers.

Acknowledgments

This work has been funded by the 6G-NTN project, which received funding from the Smart Networks and Services Joint Undertaking (SNS JU) under the European Union's Horizon Europe research and innovation programme under Grant Agreement No 101096479. The work of Daniel Gaetano Riviello was supported by the European Union—NextGenerationEU—National Recovery and Resilience Plan (Piano Nazionale di Ripresa e Resilienza, PNRR) through the Project: "SoBigData.it—Strengthening the Italian RI for Social Mining and Big Data Analytics", under Grant Prot. IR0000013—Avviso n. 3264 del 28/12/2021.

References

[1] A.Vanelli-Coralli, A. Guidotti, T. Foggi, G. Colavolpe and G. Montorsi,"5G and Beyond 5G Non-Terrestrial Networks: trends and research challenges",*IEEE 3rd 5G World Forum (5GWF), Bangalore, India*,pp.163-169, 2020.

[2] S. Kota and G. Giambene, "6G Integrated Non-Terrestrial Networks: Emerging Technologies and Challenges", *IEEE International Conference on Communications Workshops (ICC Workshops)*, Montreal, QC, Canada, pp. 1-6, 2021.

[3] V. Icolari, A. Guidotti, D. Tarchi, and A. Vanelli-Coralli, "An interference estimation technique for satellite cognitive radio systems", in 2015 *IEEE International Conference on Communications (ICC)*, 2015, pp. 892–897.

[4] S. Chatzinotas, B. Evans, A. Guidotti, V. Icolari, E. Lagunas, S. Maleki, S. K. Sharma, D. Tarchi, P. Thompson, and A. Vanelli-Coralli, "Cognitive approaches to enhance spectrum availability for satellite systems", International Journal of Satellite Communications and Networking, vol. 35, no. 5, pp. 407–442, 2017.

[5] M.R. Dakkak, D. G. Riviello, A. Guidotti, A. Vanelli-Coralli, "Evaluation of multi-user multiple-input multiple-output digital beamforming algorithms in B5G/6G low Earth orbit satellite systems", in *Int. J. Satell. Commun. Network.*, pp. 1-17, 2023.

[6] L. You, K.-X. Li, J. Wang, X. Gao, X.-G. Xia, and B. Ottersten, "Massive MIMO transmission for LEO satellite communications", *IEEE J. Sel. Areas Commun.*, vol. 38, no. 8, pp. 1851–1865, 2020.

[7] A. Guidotti and A. Vanelli-Coralli, "Clustering strategies for multicast Beamforming in multibeam satellite systems", *Int. J. Satell. Commun. Network.*, vol. 38, no. 2, pp. 85–104, 2020.

[8] ——, "Design trade-off analysis of Beamforming multi-beam satellite communication systems", in *2021 IEEE Aerospace Conference (50100)*, 2021, pp. 1–12.

[9] B. Ahmad, D. G. Riviello, A. Guidotti and A. Vanelli-Coralli, "Graph-Based User Scheduling Algorithms for LEO-MIMO Non-Terrestrial Networks," *2023 Joint European Conference on Networks and Communications & 6G Summit (EuCNC/6G Summit)*, Gothenburg, Sweden, 2023, pp. 270-275.

[10] P. Rocca, M. D'Urso and L. Poli, "Advanced Strategy for Large Antenna Array Design With Subarray-Only Amplitude and Phase Control," in *IEEE Antennas and Wireless Propagation Letters*, vol. 13, pp. 91-94, 2014.

[11] T. Isernia, M.D'Urso and O. M. Bucci, "A simple idea for an effective sub-arraying of large planar sources," *IEEE Antennas Wireless Propag. Lett.*, vol. 8, pp. 169–172, 2009.

[12] J. Yang, X. Liu, Y. Tu and W. Li, "Robust Adaptive Beamforming Algorithm for Sparse Subarray Antenna Array Based on Hierarchical Weighting, *Micromachines*, 2022, 13, 859.

[13] J. Palacios, N. Gonzalez-Prelcic, C. Mosquera, T. Shimizu, and C.-H. Wang, "A hybrid beamforming design for massive MIMO LEO satellite communications," *Frontiers in Space Technologies*, vol. 2, 2021.

[14] R. J. Mailloux, "Subarray technology for time delayed scanning arrays," in IEEE International Conference on COMCAS. IEEE, 2009, pp. 1–6.

[15] E. Castañeda, A. Silva, A. Gameiro and M. Kountouris, "An Overview on Resource Allocation Techniques for Multi-User MIMO Systems,"in IEEE Communications Surveys & Tutorials, vol. 19, no. 1, pp. 239-284, Firstquarter 2017.

[16] X. Yi and E. K. S. Au, "User Scheduling for Heterogeneous Multiuser MIMO Systems: A Subspace Viewpoint," in IEEE Transactions on Vehicular Technology, vol. 60, no. 8, pp. 4004-4013, Oct. 2011.

[17] K. -U. Storek and A. Knopp, "Fair User Grouping for Multibeam Satellites with MU-MIMO Precoding," GLOBECOM 2017 - 2017 IEEE Global Communications Conference, Singapore, 2017, pp. 1-7.

[18] M. R. Dakkak, D. G. Riviello, A. Guidotti and A. Vanelli-Coralli, "Assessment of Beamforming Algorithms with Subarrayed Planar Arrays for B5G/6G LEO Non-Terrestrial Networks", *European Wireless 2023; 28th European Wireless Conference*, Rome, Italy, 2023.

[19] B. Ahmad, D. G. Riviello, A. Guidotti and A. Vanelli-Coralli, "Improved Graph-Based User Scheduling For Sum-Rate Maximization in LEO NTN Systems", *2023 IEEE International Conference on Acoustics, Speech, and Signal Processing Workshops(ICASSPW)*, Rhodes Island, Greece, 2023, pp. 1-5.

[20] ITU-R Radiocommunication Sector of ITU, "Modelling and simulation of IMT networks and systems for use in sharing and compatibility studies (M.2101-0)", Feb. 2017.

[21] G. Alfano, C.-F. Chiasserini, A. Nordio and D. G. Riviello, "A Random Matrix Model for mmWave MIMO Systems", *Acta Phys. Pol. B*, vol. 51, no. 7, pp. 1627-1640, 2020.

[22] 3GPP, "38.821 -Solutions for NR to support Non-Terrestrial Networks (NTN)", Jun. 2021.

[23] P. Patcharamaneepakorn, S. Armour and A. Doufexi, "On the Equivalence Between SLNR and MMSE Precoding Schemes with Single-Antenna Receivers," in *IEEE Communications Letters*, vol. 16, no. 7, pp. 1034-1037, July 2012.

[24] S. Balaji, V. Swaminathan and K. Kannan, "A Simple Algorithm to Optimize Maximum Independent Set", in *Advanced Modeling and Optimization*, vol. 12, no. 1, pp-107-118, 2010.

[25] Richard L. Burden and J. Douglas Faires , *Numerical Analysis*, Cengage Learning, 10th edition, 2015.